

# On Measuring Split-SUSY Neutralino and Chargino Masses at the LHC

N. Kersting<sup>1</sup>

*Physics Department, Sichuan University, P.R. China 610065*

*and*

*Kavli Institute for Theoretical Physics, Beijing, P.R. China 100086*

## Abstract

In Split-Supersymmetry models, where the only non-Standard Model states produceable at LHC-energies consist of a gluino plus neutralinos and charginos, it is conventionally accepted that only mass *differences* among these latter are measurable at the LHC. The present work shows that application of a simple ‘Kinematic Selection’ technique allows full reconstruction of neutralino and chargino masses from one event, in principle. A Monte Carlo simulation demonstrates the feasibility of using this technique at the LHC.

---

<sup>1</sup>Email: nkersting@scu.edu.cn

# 1 Introduction

As data from the LHC is recorded and analyzed in the upcoming years, experimentalists will look for signatures of physics beyond the Standard Model (SM), in particular Supersymmetry (SUSY). The most well-studied scenario, in which SUSY alleviates the hierarchy problem with a low-energy (sub-TeV) spectrum of sparticles, entails copious production of strongly-interacting squarks and gluinos, identified via their associated jets [1, 2], which cascade through numerous decay channels involving other sparticles, including e.g. electroweak (EW)-interacting sleptons, neutralinos, and charginos — the masses of these sparticles, whose precise values are crucial to understanding features of an underlying fundamental theory, may be reconstructed (at least partially) from measurements of various invariant mass endpoints in certain exclusive decay channels (e.g. [3]). Of course it is also entirely possible that the SUSY spectrum is far above the TeV level, hence inaccessible at the LHC. In between the above two extremes, phenomenologically speaking, is the scenario where some of the sparticles are light, while others extremely massive and decoupled, “Split SUSY” [4] providing the most popular example.

At low energies, the Split-SUSY spectrum, aside from the established SM particles and one light Higgs boson, contains only four neutralinos ( $\tilde{\chi}_i^0$ ,  $i = 1..4$ ), two charginos ( $\tilde{\chi}_j^\pm$ ,  $j = 1, 2$ ), and a long-lived gluino ( $\tilde{g}$ ). The phenomenology of this latter, which would be expected to form so-called “R-hadrons” in the detector (and therefore not immediately decaying to other sparticles) has been thoroughly covered elsewhere (see [5, 6]) and will not concern us here<sup>2</sup>. The focus of the present study is rather on the neutralinos and charginos, hereafter collectively referred to as ‘EW-inos’. These cannot decay via squarks and sleptons, which are many orders of magnitude heavier, but must rather decay promptly via a Higgs or EW gauge bosons ( $Z^0$ ,  $W^\pm$ ). If mass differences between EW-inos are smaller than  $m_Z$  or  $m_W$ , they will undergo 3-body decays to quarks or leptons: e.g.  $\tilde{\chi}_i^0 \rightarrow Z^{0*}(\rightarrow \ell^\pm \ell^\mp, q\bar{q})\tilde{\chi}_1^0$ ,  $\tilde{\chi}_2^\pm \rightarrow Z^{0*}(\rightarrow \ell^\pm \ell^\mp, q\bar{q})\tilde{\chi}_1^\pm$ , and  $\tilde{\chi}_1^\pm \rightarrow W^{\pm*}(\rightarrow \ell^\pm \nu, qq')\tilde{\chi}_1^0$ . In particular, dilepton pairs from the above off-shell  $Z$  decays will have an invariant mass distribution which cuts off sharply at  $m_{\tilde{\chi}_i^0} - m_{\tilde{\chi}_1^0}$  or  $m_{\tilde{\chi}_2^\pm} - m_{\tilde{\chi}_1^\pm}$ , so the usual conclusion from Split-SUSY studies is that only mass *differences* between EW-inos are measurable at the LHC [6].

The thesis of this work is that one can do much better than just find EW-ino mass differences — the masses themselves can be reconstructed from additional kinematic analysis made possible by the fact that EW-inos must be pair-produced to preserve R-parity, which is theoretically motivated in making the lightest SUSY particle (LSP) a good dark matter candidate. Each SUSY EW-ino event ( $\tilde{\chi}_i^\pm \tilde{\chi}_j^\mp$ ,  $\tilde{\chi}_i^\pm \tilde{\chi}_j^0$ , or  $\tilde{\chi}_i^0 \tilde{\chi}_j^0$ ) may thus contain multiple (as many as ten) hard leptons, the momenta of which, when contracted into all possible invariant masses (as in [7]), encode much information. This was previously overlooked in the literature, presumably because pairs of EW-inos arising from hadronic collisions carry an uncertain center-of-mass energy, hence yielding final state leptons not amenable to the usual invariant-mass endpoint

---

<sup>2</sup>Even if the gluino does decay in some corner of parameter space, this will only assist with the current study by boosting signal rates.

analysis. As shown in Hidden Threshold (HT) methods [8], however, correlations among such invariants (i.e. a Dalitz plot) still carry information about endpoints and, more importantly for the present work, distribute events according to the kinematics in each respective EW-ino decay frame. The strategy in this work, therefore, is to focus on one region of a Dalitz plot where events must arise from the same decay frame kinematics, find the Lorentz-boosts back to the frames of the decaying EW-inos, and match energies/momenta (including measured missing transverse momenta) to extract the values of relevant masses. A single (perfect) event may suffice for full reconstruction in principle, though in practice (including detector effects and backgrounds) one must do with a collection of less-than-perfect events which will give statistical distributions of the unknown masses.

In the following, let us then proceed thusly: Section 2 will explain this ‘Kinematic Selection’ method in the context of Split-SUSY EW-ino decays; Section 3 will detail how to reconstruct EW-ino masses from a perfect event and Section 4 will then test and confirm the feasibility of this in a Monte Carlo simulation appropriate to the LHC environment. Summary and comments on further elaborations are contained in Section 5.

## 2 Kinematic Selection Technique for EW-inos

In Split-SUSY models, EW-inos at the LHC can only be pair-produced in quark-quark s-channel processes through an off-shell  $W$ ,  $Z$ , or  $\gamma$ :

$$qq' \rightarrow W^* \rightarrow \widetilde{\chi}_i^\pm \widetilde{\chi}_j^0 \quad (1)$$

$$q\bar{q} \rightarrow Z^* \rightarrow \widetilde{\chi}_i^0 \widetilde{\chi}_j^0 \quad (2)$$

$$q\bar{q} \rightarrow Z^*/\gamma^* \rightarrow \widetilde{\chi}_i^\pm \widetilde{\chi}_j^\mp \quad (3)$$

Then, since each EW-ino cannot decay through squarks or sleptons, but only through a  $Z^0$  or  $W^\pm$  (or a light higgs  $h^0$ , though this tends to be subdominant), it must decay among the following five tree-level<sup>3</sup> channels (taking  $m_{\widetilde{\chi}_1^\pm} > m_{\widetilde{\chi}_2^0}$  and  $m_{\widetilde{\chi}_2^\pm} > m_{\widetilde{\chi}_4^0}$ ):

$$\widetilde{\chi}_2^\pm \rightarrow Z^0 \widetilde{\chi}_1^\pm \quad (4)$$

$$\widetilde{\chi}_2^\pm \rightarrow W^\pm \widetilde{\chi}_i^0 \quad (i = 1..4) \quad (5)$$

$$\widetilde{\chi}_1^\pm \rightarrow W^\pm \widetilde{\chi}_i^0 \quad (i = 1, 2) \quad (6)$$

$$\widetilde{\chi}_i^0 \rightarrow Z^0 \widetilde{\chi}_j^0 \quad (i = 2..4), \quad (j = 1..i - 1) \quad (7)$$

$$\widetilde{\chi}_i^0 \rightarrow W^\pm \widetilde{\chi}_1^\mp \quad (i = 3, 4) \quad (8)$$

where the  $Z^0$  or  $W^\pm$  could be on- or off-shell. The number of possible decay chains combining (1)-(3) and (4)-(8), even without distinguishing on- or off-shell intermediaries or considering the rest of the decay chain, is already quite large, but most of these, fortunately, will not be needed in the present study.

---

<sup>3</sup>Loop-level decays can also have phenomenological importance, e.g.  $\widetilde{\chi}_i^0 \rightarrow \gamma \widetilde{\chi}_1^0$  [9].

## 2.1 Chargino-Neutralino Modes

The most heavily-produced state in Split SUSY models is likely to be a chargino-neutralino pair  $\tilde{\chi}_1^\pm \tilde{\chi}_2^0$ , since these sparticles are relatively light and well-mixed, where it is further assumed that they proceed to decay through an offshell<sup>4</sup>  $Z^0$  or  $W^\pm$  to leptons ( $\ell = e, \mu$ ):

$$\tilde{\chi}_1^\pm \rightarrow W^{\pm*} (\rightarrow \ell^\pm \nu) \tilde{\chi}_1^0 \quad (9)$$

$$\tilde{\chi}_2^0 \rightarrow Z^{0*} (\rightarrow \ell^\pm \ell^\mp) \tilde{\chi}_1^0 \quad (10)$$

The endstate will therefore contain three leptons (of which at least two are opposite-sign-same-flavor (OSSF)) whose momenta  $p_{1,2,3}$  can, in the spirit of [7], be systematically contracted into three independent invariant masses<sup>5</sup>:

$$\overline{M}_{3l}^2 \equiv (p_1 + p_2 + p_3)^2 \quad (11)$$

$$\overline{M}_{l2l}^4 \equiv \{(p_1 + p_2 - p_3)^4 + (p_3 + p_1 - p_2)^4 + (p_2 + p_3 - p_1)^4\}/3 \quad (12)$$

$$\overline{M}_{ll}^4 \equiv \{(p_1 + p_2)^4 + (p_1 + p_3)^4 + (p_2 + p_3)^4\}/3 \quad (13)$$

The problem now, in which the HT technique assists, is how to use the information contained in the above invariants to select events with a desired kinematic configuration. Observe, first of all, that the off-shell W in (1) will itself have an invariant mass somewhere (and unpredictably) in the range  $m_{\tilde{\chi}_1^\pm} + m_{\tilde{\chi}_2^0} < m^* < E_{LHC}$  where  $E_{LHC} \sim 14$  TeV is the theoretical maximum partonic collision energy at the LHC. Let us consider the case where  $m^* = m_{\tilde{\chi}_1^\pm} + m_{\tilde{\chi}_2^0}$  and designate this ‘threshold production’.

To simplify the discussion, assume we have a  $e^+e^-\mu^\pm$  endstate (the following will also pertain to same flavor states  $e^+e^-e^\pm$  or  $\mu^+\mu^-\mu^\pm$  with the correct lepton-pairing). From relativistic kinematics, it is quite straightforward to show that, for threshold production, when  $M_{e^+e^-} \equiv (p_{e^+} + p_{e^-})^2$  is *maximal*,  $\overline{M}_{l2l}$  is *minimal* when the kinematical configuration in Fig. 1a is attained: in the rest frame of the parents  $\tilde{\chi}_1^\pm$  and  $\tilde{\chi}_2^0$ , the electron and positron are produced back-to-back with maximal momentum along directions perpendicular to the muon, which also carries maximal momentum (see Appendix for derivation). The minimal value of  $\overline{M}_{l2l}$  is then given by

$$\overline{M}_{l2l}^{min} = \sqrt{m_{\tilde{\chi}_2^0} - m_{\tilde{\chi}_1^\pm}} \left( \frac{2(m_{\tilde{\chi}_2^0} - m_{\tilde{\chi}_1^\pm})^2 + (m_{\tilde{\chi}_1^\pm} - m_{\tilde{\chi}_2^0} + m_{\tilde{\chi}_1^0} - m_{\tilde{\chi}_1^0}^2/m_{\tilde{\chi}_1^\pm})^2}{3} \right)^{1/4} \quad (14)$$

(the other invariants  $M_{3l}$  and  $\overline{M}_{ll}$  are, on the contrary, trivially minimized by  $p_{\mu^\pm} = 0$ , giving  $M_{3l}^{min} = M_{e^+e^-}^{max}$  and  $\overline{M}_{ll}^{min} = (1/3)^{1/4} M_{e^+e^-}^{max}$ , respectively). For the more realistic case of non-threshold production, i.e.  $m^* > m_{\tilde{\chi}_1^\pm} + m_{\tilde{\chi}_2^0}$  giving a relative

<sup>4</sup>If decays occur through on-shell  $Z^0$  and  $W^\pm$ , the signal is much more challenging to extract, being swamped by  $WZ$  and  $ZZ$  backgrounds.

<sup>5</sup>These have the advantage of systematic definition and symmetry under lepton interchange at the cost of algebraic complexity.

velocity  $\vec{\beta}$  between the  $\tilde{\chi}_1^\pm$  and  $\tilde{\chi}_2^0$ , it is also easy to show that  $M_{e^+e^-}$  is maximal and  $\overline{M}_{l_2l}$  minimal (for *this*  $\beta$ ) for the same decay configuration (in the respective  $\tilde{\chi}_1^\pm$  and  $\tilde{\chi}_2^0$  ‘parent-frames’) of Fig. 1a. The relevant Dalitz plot is therefore “ $M_{e^+e^-}$  vs.  $\overline{M}_{l_2l}$ ”, the events of interest accumulating along where the line  $M_{e^+e^-} = M_{e^+e^-}^{max}$  ( $= m_{\tilde{\chi}_2^0} - m_{\tilde{\chi}_1^0}$ ) hits the kinematically-allowed portion of the plot<sup>6</sup>.

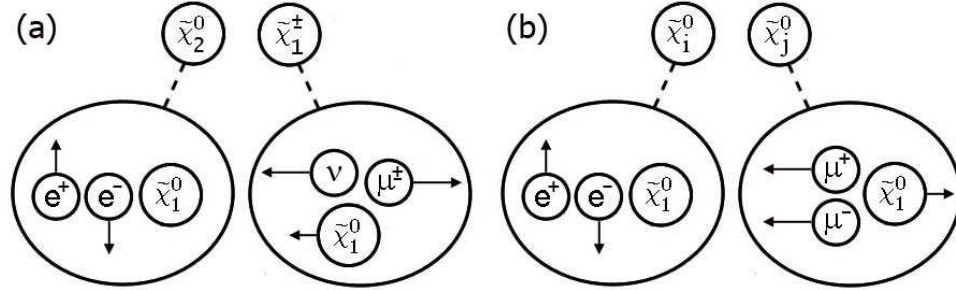


Figure 1: *Schematic of the kinematic configurations (with  $e \leftrightarrow \mu$  as well) which minimize various invariant masses at threshold for (a) Chargino-Neutralino and (b) Neutralino-Neutralino modes (these particles decay at rest in this frame).*

## 2.2 Neutralino-Neutralino Modes

Neutralino pair production (2) may also be significant, but only for *unlike* neutralinos, i.e.  $i \neq j$ , due to a suppression of the  $Z^0 \tilde{\chi}_i^0 \tilde{\chi}_j^0$  coupling [6, 10]. Assuming again that the neutralinos decay through a 3-body decay as in (10), we now have an endstate described by four lepton momenta  $p_{1,2,3,4}$  which can be analyzed via a set of seven invariant masses [7], including e.g.

$$M_{4l}^2 \equiv (p_1 + p_2 + p_3 + p_4)^2 \quad (15)$$

$$\overline{M}_{2l2l}^4 \equiv \{(p_1 + p_2 - p_3 - p_4)^4 + (p_1 + p_4 - p_2 - p_3)^4 + (p_2 + p_4 - p_1 - p_3)^4\}/3$$

Going through the same argument above for  $\tilde{\chi}_1^\pm \tilde{\chi}_2^0$  modes, one finds that the threshold kinematic configuration in Fig. 1b, where  $M_{e^+e^-}$  is maximal, forces  $M_{4l}$  and  $\overline{M}_{2l2l}$  to attain the minima (derived in Appendix)

$$M_{4l}^{min} = \sqrt{(m_{\tilde{\chi}_i^0} - m_{\tilde{\chi}_1^0})(m_{\tilde{\chi}_j^0} + m_{\tilde{\chi}_i^0} - m_{\tilde{\chi}_1^0} - m_{\tilde{\chi}_i^0}^2/m_{\tilde{\chi}_j^0})} \quad (16)$$

$$\overline{M}_{2l2l}^{min} = \sqrt{m_{\tilde{\chi}_i^0} - m_{\tilde{\chi}_1^0}} \left( \frac{2(m_{\tilde{\chi}_i^0} - m_{\tilde{\chi}_1^0})^2 + (m_{\tilde{\chi}_j^0} - m_{\tilde{\chi}_i^0} + m_{\tilde{\chi}_1^0} - m_{\tilde{\chi}_i^0}^2/m_{\tilde{\chi}_j^0})^2}{3} \right)^{1/4}$$

and events of this type can be found near these minima on a plot of  $M_{e^+e^-}$  (or  $M_{\mu^+\mu^-}$ ) versus  $M_{4l}$  and  $\overline{M}_{2l2l}$ .

<sup>6</sup>One might hope to measure the endpoint (14) from the intersection and thereby constrain SUSY masses, but this turns out to require very high (sub-GeV) endpoint precision and is much inferior to the present method.

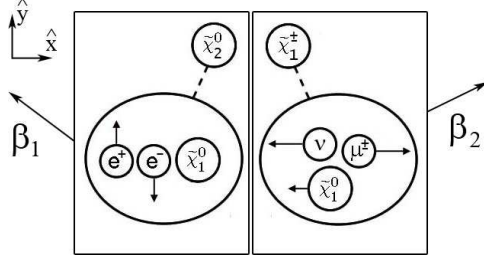


Figure 2: *Class of parent-frame kinematics sought: in the frame where the  $\tilde{\chi}_2^0$  decays at rest, the  $e^\pm$  are along global coordinates  $\pm\hat{y}$  with maximal energy; likewise in the  $\tilde{\chi}_1^\pm$  decay frame the muon is along  $\pm\hat{x}$  with maximal energy. Any velocities  $\beta_{1,2}$  of these decaying states in the lab frame are permitted.*

### 3 Finding Masses from One Event

Let us now suppose we have a  $e^+e^-\mu^\pm$  event of maximal  $M_{e^+e^-}$  and minimal  $\overline{M}_{l2l}$  (a very similar analysis can be done for  $e^+e^-\mu^+\mu^-$  events from  $\tilde{\chi}_i^0\tilde{\chi}_j^0$  decays, but we will not need this for the present study<sup>7</sup>). By the discussion of the last section the kinematic configuration must be of the type shown in Fig. 2, i.e. if the decaying  $\tilde{\chi}_2^0$  and  $\tilde{\chi}_1^\pm$  had no motion then the  $e^\pm$  would have equal and opposite momenta (along say  $\pm\hat{y}$ ) while the muon would be emitted perpendicular to  $\hat{y}$ , say along  $\hat{x}$ , also with maximal kinetic energy; the  $\tilde{\chi}_2^0$  and  $\tilde{\chi}_1^\pm$  are, however, permitted to be moving with different velocities  $\vec{\beta}_{1,2}$ , so the observed leptonic momenta will generally point in random directions.

These leptonic momenta nevertheless carry useful information, for if we knew  $\vec{\beta}_{1,2}$  as well we could reconstruct all three unknown masses  $m_{\tilde{\chi}_1^0}$ ,  $m_{\tilde{\chi}_2^0}$ , and  $m_{\tilde{\chi}_1^\pm}$  as follows: the observed missing transverse momentum  $\vec{p}_T$  must clearly arise from the invisible particles  $2\tilde{\chi}_1^0 + \nu$ , and since their 4-momenta are known functions of the masses in the  $\tilde{\chi}_2^0$  and  $\tilde{\chi}_1^\pm$  decay frames, it is a simple matter of Lorentz-boosting these by  $\vec{\beta}_{1,2}$  to the lab frame and matching to the two components of  $\vec{p}_T$ . Two matching conditions plus the dilepton edge ( $M_{e^+e^-}^{max} = m_{\tilde{\chi}_2^0} - m_{\tilde{\chi}_1^0}$ ) determines the set  $\{m_{\tilde{\chi}_1^0}, m_{\tilde{\chi}_2^0}, m_{\tilde{\chi}_1^\pm}\}$ .

It is easy, in fact, to determine  $\vec{\beta}_1$ : this corresponds to the unique Lorentz transformation  $\Lambda_1$  which makes the transformed  $e^\pm$  momenta equal and opposite ( $\equiv \pm\vec{p}'$ ), as well as simultaneously bringing the corresponding  $\tilde{\chi}_1^0$  to rest, and is given by

$$\vec{\beta}_1 = \frac{\vec{p}_{e^+} + \vec{p}_{e^-}}{E_{e^+} + E_{e^-}} \quad (17)$$

As for  $\vec{\beta}_2$ , there is no nice analytical expression, but we can nevertheless constrain

<sup>7</sup>If the number of  $e^+e^-\mu^+\mu^-$  events is sufficiently high we can also get events where  $M_{e^+e^-}$  and  $M_{\mu^+\mu^-}$  are both maximal, also allowing for a straightforward mass-reconstruction [11].

it by conservation of the total missing 4-momentum  $\vec{p}^\mu$ ,

$$\vec{p}^\mu = \Lambda_1^{-1} \begin{pmatrix} m_{\tilde{\chi}_1^0} \\ 0 \end{pmatrix} + \Lambda_2^{-1} \begin{pmatrix} m_{\tilde{\chi}_1^\pm} - E'' \\ -\vec{p}'' \end{pmatrix} \quad \left[ \begin{pmatrix} E'' \\ \vec{p}'' \end{pmatrix} \equiv \Lambda_2 \begin{pmatrix} E_{\mu^\pm} \\ \vec{p}_{\mu^\pm} \end{pmatrix} \right] \quad (18)$$

(ie. total missing 4-momentum = 4-momentum of one LSP plus 4-momentum of other LSP+ $\nu$  system) of which the two transverse components  $\vec{p}_T$  are measurable, in addition to the three kinematic constraints

$$\vec{p}' \cdot \vec{p}'' = 0 \quad , \quad E'' = \frac{m_{\tilde{\chi}_1^\pm}^2 - m_{\tilde{\chi}_1^0}^2}{2m_{\tilde{\chi}_1^\pm}} \quad , \quad M_{e^+e^-}^{max} = m_{\tilde{\chi}_2^0} - m_{\tilde{\chi}_1^0} \quad (19)$$

Thus, (18) and (19) compose a system of five equations for the six unknowns  $\{\vec{\beta}_2, m_{\tilde{\chi}_1^0}, m_{\tilde{\chi}_2^0}, m_{\tilde{\chi}_1^\pm}\}$ . If, as in a wide class of SUSY spectra (here controlled by SUSY parameters  $\mu$ ,  $M_{1,2}$ , and  $\tan\beta$ ) we have the approximate relation  $m_{\tilde{\chi}_1^\pm} \approx m_{\tilde{\chi}_2^0}$ , then we are less one unknown and the five equations can be numerically solved for the masses  $m_{\tilde{\chi}_1^0}$  and  $m_{\tilde{\chi}_2^0}$ .

## 4 Monte Carlo Test

In a real experiment, there are of course many reasons why even a ‘perfect’ event like Fig. 2 does not suffice for reliable mass reconstruction: measurement errors as well as inherent finiteness of detector resolution and sparticle widths will throw off the solution. Then there is the reality that no event is perfectly situated at an endpoint and, moreover, competition from backgrounds is expected. What we must do in practice, therefore, is to collect a number of events in some optimized neighborhood of the region of interest on the “ $M_{\ell+\ell^-}$  vs.  $\overline{M}_{l2l}$ ” plot, impose conditions (17)-(19) on each event (with  $M_{e^+e^-}^{max} \rightarrow M_{\ell+\ell^-}$  plus the assumption  $m_{\tilde{\chi}_1^\pm} \approx m_{\tilde{\chi}_2^0}$ ), and study the distribution of extracted masses  $m_{\tilde{\chi}_{1,2}^0}$  (the reader is referred to the Appendix for a more detailed discussion of the numerical solving procedure).

Let us see how this might work by running the above programme through a Monte Carlo simulation of LHC data. Suppose for definiteness that Nature has chosen the Split SUSY parameter point considered in [6] with GUT-scale parameters

$$\begin{aligned} M_1 &= M_2 = M_3 = 120 \text{ GeV} \\ \mu &= -90 \text{ GeV} \\ \tan\beta &= 4 \end{aligned}$$

in addition to a symmetry-breaking scale  $\tilde{m} = 10^9 \text{ GeV}$ . Integrating down to EW energies ( $Q = m_Z$ ), all SUSY particles decouple except for the gluino and EW-inos, which attain the spectrum shown in Table 1; this is consistent with LEP and dark-matter constraints. At LHC energies the dominant chargino-neutralino production channels would then be<sup>8</sup>  $\tilde{\chi}_1^\pm \tilde{\chi}_2^0$  ( $\sigma = 4650 \text{ fb}$ ) and  $\tilde{\chi}_1^\pm \tilde{\chi}_3^0$  ( $\sigma = 2099 \text{ fb}$ ), while the main neutralino-neutralino channel is  $\tilde{\chi}_2^0 \tilde{\chi}_3^0$  ( $\sigma = 876 \text{ fb}$ ).

---

<sup>8</sup>See [6] for a complete table of these.

Table 1: *Relevant masses (in GeV) at the Split-SUSY point we consider.*

$\tilde{\chi}_1^0$	$\tilde{\chi}_2^0$	$\tilde{\chi}_3^0$	$\tilde{\chi}_4^0$	$\tilde{\chi}_1^\pm$	$\tilde{\chi}_2^\pm$	$\tilde{g}$
71.1	109.9	141.7	213.7	114.7	215.7	807.0

LHC EW-ino events ( $pp \rightarrow \tilde{\chi}_i^0 \tilde{\chi}_j^0, \tilde{\chi}_{1,2}^\pm \tilde{\chi}_k^0, \tilde{\chi}_{1,2}^\pm \tilde{\chi}_{1,2}^\mp$ ) and SM backgrounds  $ZZ, WZ$  and  $W\gamma^*$  (see [12] and [13] for a good discussion of these and others not necessary for this study), corresponding to  $300 \text{ fb}^{-1}$  integrated luminosity are then generated via the HERWIG 6.5 package [14] and run through a simplified detector simulator<sup>9</sup>. The following cuts are then employed, depending on the number of final leptons:

**For 2-Lepton Endstates:**

- Leptons must be isolated: no tracks of other charged particles are present in a  $r = 0.3 \text{ rad}$  cone around the lepton, with less than  $3 \text{ GeV}$  of energy deposited into the electromagnetic calorimeter for  $0.05 \text{ rad} < r < 0.3 \text{ rad}$  around the lepton.
- Leptons must be sufficiently hard:  $p_T^\ell > 10, 8 \text{ GeV}$  for  $\ell = e, \mu$ .

**For 3- and 4- Lepton Endstates:**

- Leptons must be hard and isolated as for 2-lepton endstates.
- Sufficient missing energy must be present in each event:  $E_T > 50 \text{ GeV}$ .

(note: 4-lepton selection criteria are shown for completeness only; the present study does not consider them further due to smallness of rate at **this** Split SUSY point)

Though SM backgrounds are substantially reduced by these cuts, they still tend to far outnumber the SUSY signal events for 2- and 3-lepton endstates. We will see shortly there is no cause for worry, however, since SM backgrounds populate uninteresting regions of the relevant invariant mass plots, shown in Fig. 3.

First observe the large number of 2-lepton events in Fig. 3a: there are roughly  $6 \cdot 10^4$  SUSY  $\ell^+ \ell^-$  events plus  $3 \cdot 10^5$  SM events (mostly from Z decays and hence sitting near the Z-pole,  $M_{\ell^+ \ell^-} \sim 91 \pm 10 \text{ GeV}$ , not shown in the Figure) which, after subtracting wrong-flavor  $e^\pm \mu^\pm$  combinations ( $5 \cdot 10^4$  of these total), give us a dilepton invariant mass distribution that clearly identifies an endpoint at  $M_{\ell^+ \ell^-} \sim 39 \text{ GeV}$  due to  $\tilde{\chi}_2^0 \rightarrow \tilde{\chi}_1^0$  decays<sup>10</sup> (a second endpoint from  $\tilde{\chi}_3^0 \rightarrow \tilde{\chi}_1^0$  decays near  $\sim 70 \text{ GeV}$  is barely

<sup>9</sup>The set-up is the same as in several of the author's previous publications (e.g. [7, 10, 15, 16]), and includes a privately-coded fast detector response simulation incorporating all the requisite simplified-geometry calorimetry, missing energy reconstruction, lepton isolation, etc., and has been checked against results in the literature using publicly available codes.

<sup>10</sup>In this feasibility-level study, it is sufficient to mark this endpoint to within a few GeV; more complete analyses [1, 2] of dilepton distributions with comparable or lower statistics verify harmlessness of SM backgrounds and suggest sub-GeV level precision is easily attainable.



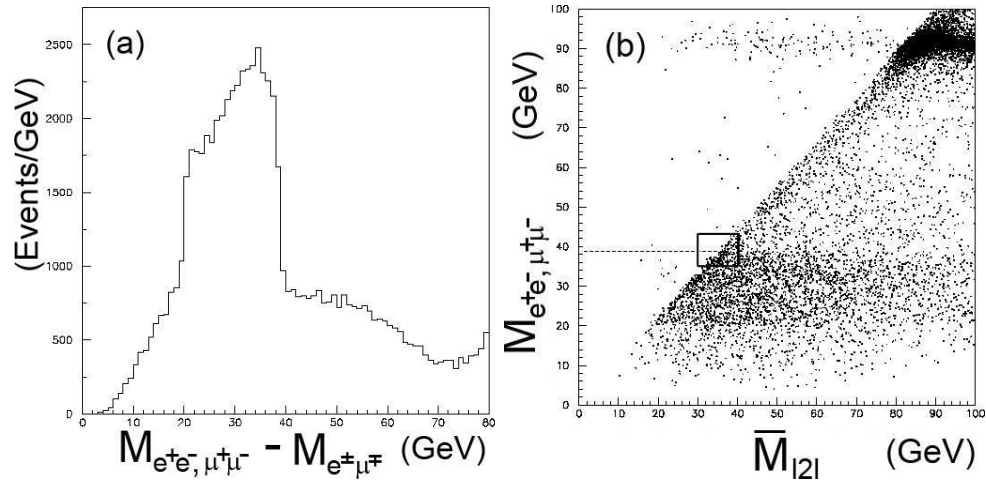


Figure 3: *Invariant mass plots for 300 fb<sup>-1</sup> luminosity (SUSY + SM): (a) The flavor-subtracted dilepton invariant mass distribution clearly identifies the endpoint at  $\sim 39$  GeV. (b) correlation between  $M_{\ell+\ell-}$  and  $\overline{M}_{|2l|}$ ; events are taken in the boxed region shown, i.e. the neighborhood of where the line  $M_{\ell+\ell-} = 39$  GeV hits the envelope.*

discernible but might be claimed statistically significant via a more in-depth analysis, e.g. [17]).<sup>11</sup>

Turning now to 3-lepton events, SUSY events ( $e^+e^-\mu^\pm + \mu^+\mu^-e^\pm$  as well as same-flavor  $e^+e^-e + \mu^+\mu^-\mu^\pm$  events<sup>12</sup>) number close to  $\sim 8000$  against a SM background several times larger, but this latter is, in the ‘ $M_{\ell+\ell-}$  vs.  $\overline{M}_{|2l|}$ ’ plot shown in Fig. 3b, concentrated mostly up near the Z-pole again, and to a much lesser extent throughout the bulk of the plot. The kinematically allowed region has a fairly clear diagonal ‘left edge’, and it is where the line  $M_{\ell+\ell-} = 39$  GeV hits this edge that we should expect events of the type in Fig. 2. Events are therefore collected from the boxed region shown, the limits of which ( $M_{\ell+\ell-} = 39 \pm 4$  GeV,  $\overline{M}_{|2l|} < 40$  GeV) give the optimal distribution of  $m_{\tilde{\chi}_1^0}$ , shown in Fig. 4a. Although this region certainly includes a large number of background events (e.g.  $\tilde{\chi}_2^0\tilde{\chi}_3^0 \rightarrow e^+e^-\mu^+\mu^-2\tilde{\chi}_1^0$ , with one of the four leptons failing the hardness cut, or  $\tilde{\chi}_2^\pm\tilde{\chi}_2^\mp \rightarrow e^+e^-\mu^\mp\nu\tilde{\chi}_1^0$ ), SM processes  $W\gamma^*$ , as well as same-flavor signal events with the wrong lepton-pairing), their presence can be tolerated since these either do not give a physically-acceptable solution to the system of equations (17)-(19), hence are rejected, or they give no *preferred* solution and lead to a uniform ‘noise’ in the  $m_{\tilde{\chi}_1^0}$ -distribution. This latter, in fact, peaks sharply (a Gaussian fit gives  $m_{\tilde{\chi}_1^0} \sim 63 \pm 3$  GeV) but somewhat lower (by about 15%) than the nominal value in Table 1 (the  $m_{\tilde{\chi}_2^0}$ -distribution looks the same but shifted by  $\sim 39$  GeV). This deviation may arise from the fact that the assumption  $m_{\tilde{\chi}_1^\pm} = m_{\tilde{\chi}_2^0}$  is inaccurate by several percent at this parameter point (see Appendix for

<sup>11</sup>There is also an ‘edge’ at  $M_{\ell+\ell-} \sim 20$  GeV, but this is actually an effect of lepton pT cuts: since two leptons with momenta  $p_\pm$  and relative angle  $\theta$  give an invariant mass of  $M_{\ell+\ell-} = \sqrt{2p_+p_-(1 - \cos\theta)}$ , cutting away  $p_\pm < 10$  GeV will tend to deplete the  $M_{\ell+\ell-}$  spectrum below  $2p_\pm = 20$  GeV.

<sup>12</sup>For same-flavor events, both possible lepton-pairings are plotted.

a discussion). If, instead, one does not make this assumption, but knows beforehand the value of  $m_{\tilde{\chi}_1^0}$  from other measurements, (17)-(19) can also be used to find  $m_{\tilde{\chi}_1^\pm}$ . The distribution shown in Fig. 4b gives the correct  $m_{\tilde{\chi}_1^\pm}$  within errors ( $m_{\tilde{\chi}_1^\pm} = 108 \pm 15$  GeV). Note this value of  $m_{\tilde{\chi}_1^\pm}$  can be put back into (17)-(19) to solve for  $m_{\tilde{\chi}_1^0}$  again, iterating the process.

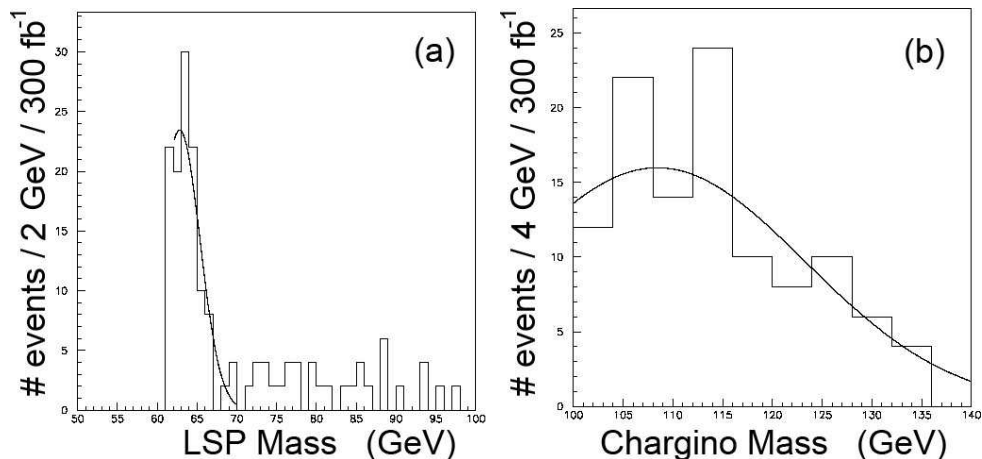


Figure 4: (a) Distribution of  $m_{\tilde{\chi}_1^0}$  from events in the boxed region of Fig. 3b, assuming  $m_{\tilde{\chi}_1^\pm} = m_{\tilde{\chi}_2^0}$ . (b) Distribution of  $m_{\tilde{\chi}_1^\pm}$  assuming the correct value of  $m_{\tilde{\chi}_1^0} = 71$  GeV. In both plots the LEP2 constraint  $m_{\tilde{\chi}_1^\pm} \geq 100$  GeV [18] has been applied.

## 5 Discussion and Conclusion

This paper has introduced a Kinematic Selection technique applicable to EW-ino pair decays where 3- or 4-lepton events with specific parent-frame kinematics are captured for analysis. Such a technique is particularly suited to Split SUSY models, where EW-inos are the only low-lying states expected to be observable at the LHC. At the specific parameter point studied, the rate of  $\tilde{\chi}_1^\pm \tilde{\chi}_2^0$ -pair decays to three leptons was sufficient to capture  $O(10^2)$  interesting events, the kinematics of which could be reconstructed well enough to extract two EW-ino masses  $m_{\tilde{\chi}_{1,2}^0}$  within 15% or so of their nominal values, assuming that  $m_{\tilde{\chi}_1^\pm} = m_{\tilde{\chi}_2^0}$ . It is, of course, entirely possible that other Split-SUSY parameter points would give higher rates and thus allow us to study  $\tilde{\chi}_2^0 \tilde{\chi}_{3,4}^0$  modes as well as those involving the heavier chargino  $\tilde{\chi}_2^\pm$  (here the kinematics are more complicated, but the final state also contains more leptons, hence more useful invariant mass constraints). Also, if EW-inos decay through an on-shell Z or W, or through a light Higgs boson, we can in principle look for leptonic invariant mass correlations which isolate events with specific parent-frame kinematics (note final state jets can also be included in this formalism); the method is quite flexible.

What other mass reconstruction methods are available for analyzing Split-SUSY EW-ino decays? First consider the neutralinos. There are now an array of methods

which take advantage of the pair-production of neutralinos. One class of “Mass-Shell Techniques” (MST), represented in the work of [19] and [20], essentially depends on maximizing the solvability of assumed mass-shell constraints in a given sample of events. This seems quite effective for on-shell decays<sup>13</sup>, but for the off-shell decay topologies in the present work these methods cannot be applied since there are not enough such constraints. Recently fashionable “transverse mass variable” methods [22, 23], e.g.  $m_{T2}$ , might be applied, though these are usually stated for symmetric decays. In one such development [24], for example, a “constrained mass variable”  $m_{2C}$  proves quite powerful for  $\tilde{\chi}_2^0\tilde{\chi}_2^0$  modes (followed by off-shell decays such as (10)); though such modes are expected to be negligible in Split-SUSY scenarios, presumably  $m_{2C}$  could be applied to the case of *unlike* neutralinos  $\tilde{\chi}_2^0\tilde{\chi}_3^0$  as well. It’s worth mentioning here that in the some of the latest developments with  $m_{T2}$ , e.g.  $m_{T2}$ -Assisted-On-Shell (MAOS) reconstruction [25], information on the full LSP 4-momentum can be gleaned for both mass and spin determination.

As for decay modes with charginos such as  $\tilde{\chi}_1^\pm\tilde{\chi}_2^0$ , the author is not aware of any work showing how to reconstruct all the unknown masses (MAOS has not yet been tested [26]) — perhaps the above techniques can encompass these modes as well, but there may be fundamental difficulties with extra invisible particles (neutrinos) in the decay products (e.g. MSTs would have too many unknown degrees of freedom in each event). Finally, there is the under-addressed question of multiple competing decay channels, e.g. when several different  $\tilde{\chi}_i^0\tilde{\chi}_j^0$  and  $\tilde{\chi}_1^\pm\tilde{\chi}_j^0$  occur with similar rates. The case of  $\tilde{\chi}_i^0\tilde{\chi}_j^0$  yielding a  $e^+e^-\mu^+\mu^-$  endstate, in particular, is subject to a wedgebox analysis [15] to partially separate events according to decay topology, though this has not been (but should be) extensively tested for mass reconstruction methods which have so far only concentrated on a single channel. Note that in the method of the current paper this separation is unnecessary, since minima such as  $\overline{M}_{l2l}^{min}$  for various channels lie on different points of the envelope in Fig. 3b. It seems quite natural that a combination of several techniques will be necessary to both isolate relatively pure samples of a given decay and reconstruct unknown masses as best as can be done at the LHC. For example, an MST-analysis might be applied to 4-lepton events from  $\tilde{\chi}_2^0\tilde{\chi}_3^0$  modes to get a ballpark estimate of  $m_{\tilde{\chi}_1^0}$ , this value then used in the current method with  $\tilde{\chi}_1^\pm\tilde{\chi}_2^0$  modes to determine  $m_{\tilde{\chi}_1^\pm}$ , as done in Fig. 4b.

In conclusion, then, this work represents the first application of a Kinematic Selection technique, found to be of particular use in Split-SUSY models. The strengths of Kinematic Selection include simplicity (relativistic kinematics) and robustness (works for multiple decay channels, even with backgrounds), which should make it a useful tool to experimentalists unraveling data from the LHC.

## Acknowledgments

This work was funded in part by the Kavli Institute for Theoretical Physics (Beijing). Thanks to A. Cohen for useful discussion relevant to the manuscript.

---

<sup>13</sup>But see [21] for some important caveats.

# Appendix

## Derivation of Minima

In Section 2 the threshold minima (14) and (16) were stated without derivation; here let us see how these were obtained.

Starting with  $\overline{M}_{l2l}$  for a  $e^+e^-\mu^\pm$  endstate, choose the threshold frame of reference to be such that the electron/positron (of maximal invariant mass) are emitted along the z-axis  $\pm\hat{z}$ , while the muon (with maximal energy) is produced at spherical angles  $\theta, \phi$ :

$$p_{e^\pm}^\mu = \begin{pmatrix} E \\ 0 \\ 0 \\ \pm E \end{pmatrix}, \quad p_{\mu^\pm}^\mu = \begin{pmatrix} E'' \\ E'' \sin \theta \cos \phi \\ E'' \sin \theta \sin \phi \\ E'' \cos \theta \end{pmatrix} \quad \left[ E \equiv \frac{m_{\tilde{\chi}_2^0} - m_{\tilde{\chi}_1^0}}{2}, \quad E'' \equiv \frac{m_{\tilde{\chi}_1^\pm}^2 - m_{\tilde{\chi}_1^0}^2}{2m_{\tilde{\chi}_1^\pm}} \right]$$

Plugging these four-vectors into the definition of  $\overline{M}_{l2l}$  in (13) and simplifying a bit, one obtains

$$\begin{aligned} \overline{M}_{l2l} = \sqrt{\frac{m_{\tilde{\chi}_2^0} - m_{\tilde{\chi}_1^0}}{\sqrt{3}m_{\tilde{\chi}_1^\pm}}} (2m_{\tilde{\chi}_1^0}^4 - 2m_{\tilde{\chi}_1^0}^3 m_{\tilde{\chi}_1^\pm} + m_{\tilde{\chi}_1^0}^2 m_{\tilde{\chi}_1^\pm}^2 (2m_{\tilde{\chi}_2^0} - m_{\tilde{\chi}_1^\pm}) + 2m_{\tilde{\chi}_1^0} m_{\tilde{\chi}_1^\pm}^2 (m_{\tilde{\chi}_1^\pm} - 3m_{\tilde{\chi}_2^0}) \\ + m_{\tilde{\chi}_1^\pm}^2 (2m_{\tilde{\chi}_1^\pm} + 3m_{\tilde{\chi}_2^0} - 2m_{\tilde{\chi}_2^0} m_{\tilde{\chi}_1^\pm}) + (m_{\tilde{\chi}_1^\pm} - m_{\tilde{\chi}_1^0})^2 \cos 2\theta)^{1/4} \end{aligned}$$

This is clearly minimal when  $\theta = \pi/2$ , and further algebraic simplification leads to (14).

With a four-lepton endstate like  $e^+e^-\mu^+\mu^-$ , where the  $e^+e^-$  pair, say, has maximal invariant mass along the z-axis, one muon ( $\mu^+$ ) will be going at an angle  $\theta_+$  to the z-axis, while the other ( $\mu^-$ ) has its own spherical angles  $\theta_-, \phi$ :

$$p_{e^\pm}^\mu = \begin{pmatrix} E \\ 0 \\ 0 \\ \pm E \end{pmatrix}, \quad p_{\mu^+}^\mu = \begin{pmatrix} E_+ \\ E_+ \sin \theta_+ \\ 0 \\ E_+ \cos \theta_+ \end{pmatrix}, \quad p_{\mu^-}^\mu = \begin{pmatrix} E_- \\ E_- \sin \theta_- \cos \phi \\ E_- \sin \theta_- \sin \phi \\ E_- \cos \theta_- \end{pmatrix}$$

where the energies  $E_\pm$  take on a range of values determined by the relative angle between the muons and 3-body kinematics. One *could* then plug these expressions into the definitions of, e.g.,  $M_{4l}$  and  $\overline{M}_{2l2l}$  and minimize over the angles, but it's much faster to intuit that since we're interested in minimizing an invariant mass, the muons should be going in the same direction ( $\theta_+ = \theta_-$  and  $\phi = 0$ ) which forces  $E_+ = E_- = (m_{\tilde{\chi}_3^0}^2 - m_{\tilde{\chi}_1^0}^2)/2m_{\tilde{\chi}_3^0}$ ; plugging this into the definitions (15) and simplifying yields the quoted minima (16), and numerically sampling over  $(\theta_+, \theta_-, \phi)$ -space confirms these are indeed correct.

## Numerically Solving for the Masses

The most direct method of numerically solving the system of equations (18) and (19) for the variables  $\{\beta_{2x}, \beta_{2y}, \beta_{2z}, m_{\tilde{\chi}_1^0}, m_{\tilde{\chi}_2^0}, m_{\tilde{\chi}_1^\pm}\}$  (where, say,  $m_{\tilde{\chi}_1^0}$  is known) is to

simply loop over a liberal range of values for  $m_{\tilde{\chi}_1^\pm}$  (say between 50 GeV and 300 GeV) and the components of  $\vec{\beta}_2$  ( $\beta_{2x,y,z}$  each between -1 and 1, with  $|\vec{\beta}_2| < 1$ ), imposing the other constraints inside these four nested loops. In fact, we only need to loop over two of the components of  $\vec{\beta}_2$ , since the third is fixed by a requirement on the transformed muon energy: when the muon four-momentum  $p_\nu$  is boosted back to the chargino's decay frame by  $\vec{\beta}_2$ , i.e.

$$\begin{pmatrix} E'' \\ p_x'' \\ p_y'' \\ p_z'' \end{pmatrix} = \begin{pmatrix} \gamma_2 & \beta_{2x}\gamma_2 & \beta_{2y}\gamma_2 & \beta_{2z}\gamma_2 \\ \beta_{2x}\gamma_2 & 1 + (\gamma_2 - 1)\frac{\beta_{2x}^2}{\beta_2^2} & (\gamma_2 - 1)\frac{\beta_{2x}\beta_{2y}}{\beta_2^2} & (\gamma_2 - 1)\frac{\beta_{2x}\beta_{2z}}{\beta_2^2} \\ \beta_{2y}\gamma_2 & (\gamma_2 - 1)\frac{\beta_{2x}\beta_{2y}}{\beta_2^2} & 1 + (\gamma_2 - 1)\frac{\beta_{2y}^2}{\beta_2^2} & (\gamma_2 - 1)\frac{\beta_{2y}\beta_{2z}}{\beta_2^2} \\ \beta_{2z}\gamma_2 & (\gamma_2 - 1)\frac{\beta_{2x}\beta_{2z}}{\beta_2^2} & (\gamma_2 - 1)\frac{\beta_{2y}\beta_{2z}}{\beta_2^2} & 1 + (\gamma_2 - 1)\frac{\beta_{2z}^2}{\beta_2^2} \end{pmatrix} \begin{pmatrix} E \\ p_x \\ p_y \\ p_z \end{pmatrix}$$

we must satisfy the constraint from 3-body kinematics,

$$E'' = \frac{m_{\tilde{\chi}_1^\pm}^2 - m_{\tilde{\chi}_1^0}^2}{2m_{\tilde{\chi}_1^\pm}} = \frac{E - \beta_{2x}p_x - \beta_{2y}p_y - \beta_{2z}p_z}{\sqrt{1 - \beta_{2x}^2 - \beta_{2y}^2 - \beta_{2z}^2}}$$

This can be rearranged into a quadratic equation for  $\beta_{2x}$ ,

$$0 = A\beta_{2x}^2 + B\beta_{2x} + C \quad (20)$$

where

$$\begin{aligned} A &\equiv 1 + (p_x/E'')^2 \\ B &\equiv -2(p_x/E'')(E/E'' - p_y/E''\beta_{2y} - p_z/E''\beta_{2z}) \\ C &\equiv \beta_{2y}^2 + \beta_{2z}^2 - 1 + (E/E'' - p_y/E''\beta_{2y} - p_z/E''\beta_{2z})^2 \end{aligned}$$

There is of course a potentially two-fold ambiguity in the solution for  $\beta_{2x}$ , and both values must be tried (if they are indeed real and satisfy  $|\beta_2| < 1$ ). Scanning over the 3-dimensional  $(m_{\tilde{\chi}_1^\pm}, \beta_{2y}, \beta_{2z})$ -space then, we look for the point which best satisfies the missing-momentum constraints (these must be satisfied within  $\pm 10$  GeV) as well as the kinematic constraint  $\vec{p}' \cdot \vec{p}'' = 0$ , achieved by minimizing  $\Delta$ :

$$\begin{aligned} \Delta &\equiv \sqrt{\Delta_1^2 + \Delta_2^2 + \Delta_3^2} \\ \Delta_1 &\equiv \vec{p}^x + \beta_{1x}\gamma_1 m_{\tilde{\chi}_1^0} + \\ &\quad \beta_{2x}\gamma_2(m_{\tilde{\chi}_1^\pm} - E'') - (1 + (\gamma_2 - 1)\frac{\beta_{2x}^2}{\beta_2^2})p_x'' - (\gamma_2 - 1)\frac{\beta_{2x}\beta_{2y}}{\beta_2^2}p_y'' - (\gamma_2 - 1)\frac{\beta_{2x}\beta_{2z}}{\beta_2^2}p_z'' \\ \Delta_2 &\equiv \vec{p}^y + \beta_{1y}\gamma_1 m_{\tilde{\chi}_1^0} + \\ &\quad \beta_{2y}\gamma_2(m_{\tilde{\chi}_1^\pm} - E'') - (1 + (\gamma_2 - 1)\frac{\beta_{2y}^2}{\beta_2^2})p_y'' - (\gamma_2 - 1)\frac{\beta_{2x}\beta_{2y}}{\beta_2^2}p_x'' - (\gamma_2 - 1)\frac{\beta_{2y}\beta_{2z}}{\beta_2^2}p_z'' \\ \Delta_3 &\equiv \alpha(\vec{p}' \cdot \vec{p}'')/(|\vec{p}'||\vec{p}''|) \end{aligned}$$

where  $\beta_1$  is already known from (17), and  $\alpha$  is a weight (high  $\alpha \sim 1000$  seems best, meaning that all solutions have essentially perpendicular leptons,  $|\cos\theta| < 0.01$ ): this

minimization always gave a unique solution in all cases tested. Moreover, this procedure is efficient in dealing with backgrounds (or same-flavor  $e^+e^-e^\pm$  and  $\mu^+\mu^-\mu^\pm$  events with the wrong lepton-pairing): either these fail to satisfy both missing energy constraints ( $\Delta_{1,2}$ ) within  $\pm 10$  GeV, or yield solutions randomly distributed across mass space, which merely provides a uniform 'noise' in the solution histogram.

The same algorithm applies, of course, when  $m_{\tilde{\chi}_1^\pm}$  is not known (so we loop over *it*) but we assume  $m_{\tilde{\chi}_1^\pm} = m_{\tilde{\chi}_2^0}$ . Here, however, since actual kinematic data comes from an event where this equality does not strictly hold, we expect the result of the numerical solution above to have a systematic error: setting  $m_{\tilde{\chi}_1^\pm} = m_{\tilde{\chi}_2^0} + \epsilon$ , the numerical solution  $m'_{\tilde{\chi}_1^\pm}$  is offset from the actual value,  $m'_{\tilde{\chi}_1^\pm} = m_{\tilde{\chi}_1^\pm} + \delta$ . To quantitatively understand the relationship between  $\delta$  and  $\epsilon$ , we would be best off running many simulations at different Split-SUSY parameter points and plotting the correlation ' $\delta$ -versus- $\epsilon$ '; but since this is extremely time-intensive and not practical for the present work, we can get a quick-and-rough idea in the perturbative limit ( $\delta, \epsilon \ll m_{\tilde{\chi}_1^0}$ ) by letting  $(m'_{\tilde{\chi}_1^0}, m'_{\tilde{\chi}_1^\pm}, m'_{\tilde{\chi}_2^0})$  and  $(m_{\tilde{\chi}_1^0}, m_{\tilde{\chi}_1^\pm}, m_{\tilde{\chi}_2^0})$  both solve  $\Delta_1 = 0$  for the same Lorentz boosts, where

$$\begin{aligned} m_{\tilde{\chi}_1^\pm} &= m_{\tilde{\chi}_2^0} + \epsilon \\ m'_{\tilde{\chi}_1^0} &= m_{\tilde{\chi}_1^0} + \delta \\ m'_{\tilde{\chi}_1^\pm} &= m'_{\tilde{\chi}_2^0} = m_{\tilde{\chi}_2^0} + \delta \end{aligned} \quad (21)$$

and then seeing what the relationship between  $\delta$  and  $\epsilon$  must be. Thus, the exact and approximate solutions, respectively, satisfy

$$0 = \not{p}^x + \beta_{1x}\gamma_1 m_{\tilde{\chi}_1^0} + \beta_{2x}\gamma_2 \frac{m_{\tilde{\chi}_1^\pm}^2 - m_{\tilde{\chi}_1^0}^2}{2m_{\tilde{\chi}_1^\pm}} + \Omega \quad (22)$$

$$0 = \not{p}^x + \beta_{1x}\gamma_1 m'_{\tilde{\chi}_1^0} + \beta_{2x}\gamma_2 \frac{m_{\tilde{\chi}_1^\pm}^2 - m_{\tilde{\chi}_1^0}^2}{2m'_{\tilde{\chi}_1^\pm}} + \Omega \quad (23)$$

where

$$\Omega \equiv -(1 + (\gamma_2 - 1) \frac{\beta_{2x}^2}{\beta_2^2}) p_x'' - (\gamma_2 - 1) \frac{\beta_{2x}\beta_{2y}}{\beta_2^2} p_y'' - (\gamma_2 - 1) \frac{\beta_{2y}\beta_{2z}}{\beta_2^2} p_z''$$

Explicitly inserting the  $\delta$ - and  $\epsilon$ -dependencies from (21) into (22) and (23) and setting these latter equal,

$$\beta_{1x}\gamma_1 m_{\tilde{\chi}_1^0} + \beta_{2x}\gamma_2 \frac{m_{\tilde{\chi}_1^\pm}^2 - m_{\tilde{\chi}_1^0}^2}{2m_{\tilde{\chi}_1^\pm}} = \beta_{1x}\gamma_1 m'_{\tilde{\chi}_1^0} + \beta_{2x}\gamma_2 \frac{m_{\tilde{\chi}_1^\pm}^2 - m_{\tilde{\chi}_1^0}^2}{2m'_{\tilde{\chi}_1^\pm}}$$

$\Rightarrow$

$$\beta_{1x}\gamma_1 m_{\tilde{\chi}_1^0} + \beta_{2x}\gamma_2 \frac{(m_{\tilde{\chi}_2^0} + \epsilon)^2 - m_{\tilde{\chi}_1^0}^2}{2(m_{\tilde{\chi}_2^0} + \epsilon)} = \beta_{1x}\gamma_1 (m_{\tilde{\chi}_1^0} + \delta) + \beta_{2x}\gamma_2 \frac{(m_{\tilde{\chi}_2^0} + \delta)^2 - (m_{\tilde{\chi}_1^0} + \delta)^2}{2(m_{\tilde{\chi}_2^0} + \delta)}$$

And now expanding and keeping only terms of  $O(\delta)$  or  $O(\epsilon)$ , we finally arrive at

$$\delta \approx \left( \frac{1+r^2}{\frac{2\beta_{1x}\gamma_1}{\beta_{2x}\gamma_2} + (1-r)^2} \right) \epsilon \quad \left[ r \equiv \frac{m_{\tilde{\chi}_1^0}}{m_{\tilde{\chi}_2^0}} \right] \quad (24)$$

From (24) we see that, even in this greatly simplified treatment, the sign and magnitude of the correlation between  $\delta$  and  $\epsilon$  depends on the Lorentz boosts  $\vec{\beta}_{1,2}$  specific to each event. All things being equal, however,  $\beta_{1x}\gamma_1 \approx -\beta_{2x}\gamma_2$  (the  $\tilde{\chi}_2^0$  and  $\tilde{\chi}_1^\pm$  may tend to go in opposite directions), we can drop the smallish  $r$ -dependent terms, and we might thus expect a negative correlation  $\delta \approx -\epsilon$ . This is indeed what is observed at the Split-SUSY point in the present study, where  $\delta \approx -8 \text{ GeV}$  and  $\epsilon \approx 5 \text{ GeV}$ .

## References

- [1] ATLAS Detector and Physics Performance Technical Design Report 2, Chapter 20, CERN-LHCC-99-015, ATLAS-TDR-15, May, 1999, <http://atlas.web.cern.ch/Atlas/GROUPS/PHYSICS/TDR/access.html>
- [2] CMS Physics TDR 8.2 Volume II: Physics Performance, CERN/LHCC 2006-021.
- [3] H. Bachacou, I. Hinchliffe, and F. E. Paige, “Measurements of masses in SUGRA models at LHC.” *Phys.Rev.***D62**:015009 (2000); E. Lytken, “Derivation of some kinematical formulas in SUSY decay chains.” ATLAS note ATL-PHYS-COM-2004-001; J. M. Butterworth, J. Ellis and A. R. Raklev, “Reconstructing sparticle mass spectra using hadronic decays.” *JHEP* **0705**, 033 (2007); B.K. Gjelsten , D.J. Miller , and P. Osland. “Measurement of the gluino mass via cascade decays for SPS 1a.” *JHEP* **0506**:015 (2005); P. Huang, N. Kersting, and H.H. Yang, “Extracting MSSM Masses From Heavy Higgs Decays to Four Leptons at the LHC.” *Phys. Rev.* **D77**, 075011 (2008).
- [4] G.F. Giudice and A. Romanino, “Split Supersymmetry .” *Nucl.Phys.* **B699**, 65-89 (2004); N. Arkani-Hamed and S. Dimopoulos, “Supersymmetric Unification Without Low Energy Supersymmetry And Signatures for Fine-Tuning at the LHC.” *JHEP***0506**, 073 (2005).
- [5] A. Arvanitaki et al., “Limits on Split Supersymmetry from Gluino Cosmology,” *Phys.Rev.* **D72**, 075011 (2005); P. Gambino, G. F. Giudice, and P. Slavich, “Gluino Decays in Split Supersymmetry,” *Nucl.Phys.* **B726** , 35-52 (2005); K. Cheung and W. Y. Keung, “Gravitino dark matter from gluino late decay in split supersymmetry,” *Phys.Rev.* **D72**, 077701 (2005); F. Wang, W. Wang, and J. M. Yang, “Gravitino dark matter from gluino late decay in split supersymmetry,” *Phys.Rev.* **D72**, 077701 (2005); J. L. Hewett et al., “Signatures of long-lived gluinos in split supersymmetry,” *JHEP* **0409**, 070 (2004).
- [6] W. Kilian, T. Plehn, P. Richardson, and E. Schmidt, “Split Supersymmetry at Colliders,” *Eur.Phys.J.* **C39** , 229-243 (2005); also see Proceedings of 2005

International Linear Collider Workshop (LCWS 2005), Stanford, California, 18-22 Mar 2005, pp 0205. hep-ph/0507137.

- [7] P. Huang, N. Kersting and H.H. Yang, “Extracting MSSM masses from heavy Higgs boson decays to four leptons at the CERN LHC,” *Phys.Rev.***D77**, 075011 (2008).
- [8] P. Huang, N. Kersting and H.H. Yang, “Hidden thresholds: A technique for reconstructing new physics masses at hadron colliders,” arXiv:0802.0022 [hep-ph].
- [9] K. Cheung and J. Song, “Hadronic production and decays of charginos and neutralinos in split supersymmetry,” *Phys.Rev.***D72**,055019 (2005).
- [10] G. Bian *et al.*, “Wedgebox analysis of four-lepton events from neutralino pair production at the LHC,” *Eur.Phys.J.***C53**, 429 (2008).
- [11] N. Kersting, S. Kraml, A. Raklev, and M. White. Work in progress.
- [12] W. Vandelli, “Prospects for the detection of chargino-neutralino direct production with the ATLAS detector at the LHC,” CERN-THESIS-2007-072.
- [13] Z. Sullivan and E. L. Berger, “Trilepton Production at the LHC - Standard Model Sources and Beyond,” *Phys.Rev.***D78**, 034030 (2008)
- [14] G. Corcella *et al.*, *JHEP* **0101**: 010 (2001); S. Moretti, K. Odagiri, P. Richardson, M.H. Seymour and B.R. Webber, *JHEP* **0204**: 028 (2002).
- [15] M. Bisset *et al.*, “Pair-produced heavy particle topologies: MSSM neutralino properties at the LHC from gluino/squark cascade decays,” *Eur.Phys.J.***C45**, 477 (2006).
- [16] M. Bisset, N. Kersting, J. Li, S. Moretti and F. Moortgat, “Four-Lepton Signatures at the LHC of heavy neutral MSSM Higgs Bosons via Decays into Neutralino/Chargino Pairs.” in The Higgs working group: Summary report 2003. Les Houches 2003, Physics at TeV colliders, pg 108-113. hep-ph/0406152.
- [17] N. Mohr, “Neutralino Reconstruction in Dilepton Final States with the CMS Experiment,” Diplomarbeit in Physik (2008).
- [18] G. Benelli, Search for stable and long lived heavy charged particles in electron positron collisions at center of mass energies from 130-GeV to 209-GeV with the OPAL detector at LEP, UMI-31-09638 (2003)
- [19] K. Kawagoe, M. M. Nojiri and G. Polesello, “A new SUSY mass reconstruction method at the CERN LHC,” *Phys.Rev.***D71**, 035008 (2005).
- [20] H.-C. Cheng *et al.*, “Mass determination in SUSY-like events with missing energy,” *JHEP* **0712**, 076 (2007).



- [21] M. Bisset, N. Kersting, and R. Lu, “Improving SUSY Spectrum Determinations at the LHC with Wedgebox and Hidden Threshold Techniques,” arXiv:0806.2492 [hep-ph].
- [22] C. G. Lester and D. J. Summers, “Measuring masses of semi-invisibly decaying particles pair produced at hadron colliders,” Phys.Lett.**B463**, 99 (1999); A. Barr, C. Lester and P. Stephens, “ $m(T2)$ : The truth behind the glamour,” J. Phys.**G29**, 2343 (2003).
- [23] W. S. Cho et al., “Measuring superparticle masses at hadron collider using the transverse mass kink,” JHEP **0802**, 035 (2008), Phys. Rev. Lett. **100**, 171801 (2008); A. J. Barr, B. Gripaios and C. G. Lester, “Weighing WIMPS with kinks at colliders: invisible particle mass measurements from endpoints,” JHEP **0802**, 014 (2008); M. M. Nojiri et al., “Inclusive transverse mass analysis for squark and gluino mass determination,” JHEP **0806**, 035 (2008).
- [24] A. Barr, G. G. Ross, and M. Serna, “The Precision Determination of Invisible-Particle Masses at the LHC,” Phys.Rev.**D78**, 056006 (2008).
- [25] W. S. Cho et al., “ $M(T2)$ -assisted on-shell reconstruction of missing momenta and its application to spin measurement at the LHC,” arXiv:0810.4853 [hep-ph].
- [26] W. S. Cho and K. Choi, private communication.